Predicting the Onset of Ischemic Stroke With Fast High-Resolution 3D MR Spectroscopic Imaging

Zengping Lin, MSc,[1] [ORCID] Ziyu Meng, BEng,[1] Tianyao Wang, BMed,[2] Rong Guo, PhD,[3,4]
Yibo Zhao, MSc,[3,5] Yudu Li, PhD,[3,5] Bin Bo, PhD,[1] Yue Guan, PhD,[1] Jun Liu, MD,[2]
Hong Zhou, MD,[6] Xin Yu, ScD,[7] David J. Lin, MD,[8] Zhi-Pei Liang, PhD,[3,5]
Parashkev Nachev, PhD, MRCP,[9] and Yao Li, PhD[1]*

Background: Neurometabolite concentrations provide a direct index of infarction progression in stroke. However, their relationship with stroke onset time remains unclear.

Purpose: To assess the temporal dynamics of *N*-acetylaspartate (NAA), creatine, choline, and lactate and estimate their value in predicting early (<6 hours) vs. late (6–24 hours) hyperacute stroke groups.

Study Type: Cross-sectional cohort.

Population: A total of 73 ischemic stroke patients scanned at 1.8–302.5 hours after symptom onset, including 25 patients with follow-up scans.

Field Strength/Sequence: A 3 T/magnetization-prepared rapid acquisition gradient echo sequence for anatomical imaging, diffusion-weighted imaging and fluid-attenuated inversion recovery imaging for lesion delineation, and 3D MR spectroscopic imaging (MRSI) for neurometabolic mapping.

Assessment: Patients were divided into hyperacute (0–24 hours), acute (24 hours to 1 week), and subacute (1–2 weeks) groups, and into early (<6 hours) and late (6–24 hours) hyperacute groups. Bayesian logistic regression was used to compare classification performance between early and late hyperacute groups by using different combinations of neurometabolites as inputs.

Statistical Tests: Linear mixed effects modeling was applied for group-wise comparisons between NAA, creatine, choline, and lactate. Pearson's correlation analysis was used for neurometabolites vs. time. $P < 0.05$ was considered statistically significant.

Results: Lesional NAA and creatine were significantly lower in subacute than in acute stroke. The main effects of time were shown on NAA ($F = 14.321$) and creatine ($F = 12.261$). NAA was significantly lower in late than early hyperacute patients, and was inversely related to time from symptom onset across both groups ($r = -0.440$). The decrease of NAA and increase of lactate were correlated with lesion volume (NAA: $r = -0.472$; lactate: $r = 0.366$) in hyperacute stroke. Discrimination was improved by combining NAA, creatine, and choline signals (area under the curve [AUC] = 0.90).

Data Conclusion: High-resolution 3D MRSI effectively assessed the neurometabolite changes and discriminated early and late hyperacute stroke lesions.

Evidence Level: 1.

Technical Efficacy: Stage 2.

Effective management of stroke relies on accurate and efficient diagnostic tools to monitor brain ischemia and tissue damage.[1] MR techniques, such as diffusion-weighted imaging (DWI), are widely used in acute stroke management because they are sensitive for the early detection of ischemic lesions but provide no specific information about the biochemical changes within the lesion.[2,3] Developing novel neuroimaging techniques to directly define the biological characteristics of infarcts and to establish the duration and extent of tissue damage is of great importance for a better understanding of the pathophysiological mechanisms, optimizing current acute stroke therapies, and designing new therapies for tissue salvage.[4,5]

Neurometabolite concentrations provide a direct index of the progression of brain tissue injury over time because they are a direct consequence of the pathologic cascade that follows brain ischemia, including disrupted metabolism and cellular energy supplies, postischemic inflammation and final death of neurons and glial cells to form brain infarction.[6–8] MR spectroscopic imaging (MRSI) is a potentially powerful tool for noninvasive measurement of regional neurometabolite changes in stroke.[9–11] Proton MRSI can simultaneously measure N-acetylaspartate (NAA) as a marker of neuronal integrity, creatine as a marker of energy metabolism, choline as a marker of cell membrane turnover, and lactate as a marker of anaerobic glycolysis.[9] The time-dependent changes of these neurometabolites within ischemic lesions in the subacute period have been previously demonstrated in clinical settings.[10,12–15] However, partial volume effects arising from the poor spatial resolution of previous studies (over 10 mm for single slice chemical shift imaging) have thus far limited the sensitivity of MRSI, and long acquisition time (over 15 minutes for a single slice) has obstructed its clinical translation.[10,16–18] Furthermore, the temporal relationships between the time of onset and neurometabolite concentrations in the acute stroke remain to be established in a clinical context.

A fast, high-resolution 3D MRSI technique named SPICE (SPectroscopic Imaging by exploiting spatiospectral CorrElation)[19–23] was shown to enable near whole-brain neurometabolite mapping at $2.0 \times 3.0 \times 3.0$ mm^3 nominal resolution in patients presenting with acute stroke.[11] This is a substantial improvement on the previous state of the art: $5.6 \times 5.6 \times 15$ mm^3 resolution using echo-planar spectroscopic imaging (EPSI) sequence[24,25] at 3 T in 8 minutes. The SPICE technique has several novel data acquisition and processing features, including: 1) elimination of water and lipid suppression pulses to enable fast imaging; 2) use of free induction decay (FID)-based acquisition with ultrashort echo time (1.6 msec) and short repetition time (160 msec); 3) use of variable-density sampling of the (k, t)-space in EPSI-based trajectories for rapid spatiotemporal encoding; 4) acquisition of navigators for tracking and correction of magnetic field drift and patient motion; and 5) processing and reconstruction of the spatiospectral functions of different molecules from the acquired MRSI data based on a union-of-subspaces model with prelearned spectral basis functions.[19–23] Spectral quantification is performed using an improved LCModel-based algorithm that incorporated both spatial and spectral priors[23]. The previous feasibility study showed that SPICE could capture the NAA and lactate signal changes within hypoperfusion areas compared with the contralateral regions in acute (<24 hours) stroke patients, but its relationship to stroke onset time remains to be explored.

The main goal of this study was to investigate the temporal changes of neurometabolite concentrations within ischemic lesions—NAA, creatine, choline, and lactate in both acute (0–1 week) and subacute (1–2 weeks) stroke patients and to assess the extent to which the combination of all neurometabolite signals measured by 3D MRSI could discriminate between early (<6 hours) and late hyperacute (6–24 hours) stroke patients.[3]

Methods

Patients
The study was approved by the Institutional Review Board. Written informed consents were obtained from all participants or their designees. We prospectively recruited 100 patients with ischemic stroke of known onset within 2 weeks of presentation, regardless of age or stroke severity. Patients with ischemic stroke were included in this study if they had a clinically confirmed ischemic stroke; they had a 3D-MRSI scan; there was no contra-indication to MR imaging. Exclusion criteria include the presence of contraindications for MRI, intracerebral hemorrhage, nonstroke lesions on structural MRI, lesions located within white matter hyperintensities, or unknown time of onset. Twenty-seven patients were excluded (two with hemorrhagic lesions; six with preexisting lesions; six with no visible lesions; four with excessive motion corruption; two not able to finish scanning; seven with lesions inside white matter hyperintensity regions). Seventy-three patients (23 females and 50 males; mean age: 65 ± 14 years) were included in this study. All patients underwent at least one MRI scan and the median symptom onset time to the first scan was 30.1 (interquartile range [IQR], 12.8–66.6) hours. Twenty-five patients underwent a follow-up MRI scan at 29.8–322.5 hours after onset. All clinical decisions such as administration of thrombolysis were made prior to initial scanning. Seven patients received thrombolytic treatment.

MRI and ^{1}H-MRSI Protocols
Imaging was performed on a 3 T Siemens Skyra MR scanner with a standard 20-channel head and neck coil. The structural MR image acquisition protocol included 3D

magnetization-prepared rapid acquisition gradient echo (MPRAGE) imaging (repetition time [TR]/echo time [TE]/inversion time [TI] = 2400/2.13/1100 msec, spatial resolution = $1.0 \times 1.0 \times 1.0$ mm^3, field of view (FOV) = 256 mm, 192 slices), DWI (TR/TE = 5200/64 ms, spatial resolution = $1.3 \times 1.3 \times 4.0$ mm^3, FOV = 240 mm, 25 slices, $b = 0$ and $b = 1000$ sec/mm^2), and 3D fluid-attenuated inversion recovery (FLAIR) imaging (TR/TE = 9000/89 msec, spatial resolution = $0.5 \times 0.5 \times 2.0$ mm^3, FOV = 240 mm, 82 slices).

Higher resolution 3D MRSI scans were performed using SPICE.[19–23] The acquisition parameters were as follows: TR = 160 msec, TE = 1.6 msec, spatial resolution = $2.0 \times 3.0 \times 3.0$ mm^3, FOV = $240 \times 240 \times 72$ mm^3, scan time = 8 minutes. A detailed description of SPICE can be found in the previous work.[19–23] The estimated metabolite concentrations were normalized using the water reference to compensate for the B_1 inhomogeneity in the acquisition.

Lesion Segmentation and Image Registration

For the images acquired within 1 week after symptom onset, the ischemic lesion area was manually delineated by a neuroradiologist (T.W. with 10 years of experience), including voxels with increased intensity on DWI ($b = 1000$ sec/mm^2). For the images acquired more than 1 week after symptom onset, the ischemic lesions were delineated manually on the FLAIR images. The ADC, DWI, FLAIR maps, and the corresponding lesion masks were all registered to the MRSI images (metabolic maps) using affine linear transformation with 12 degrees of

TABLE 1. Demographic Data ($n = 73$)	
Mean age (SD), years	65 (13.5)
Female sex, %	31.5
Hypertension, %	79.2
Atrial fibrillation, %	11.3
Diabetes mellitus, %	32.4
Hypercholesterolemia, %	11.3
Cigarette smoker (current), %	40.9
Median NIHSS (IQR)	4 (3–8)
Median lesion volume at the first scan (IQR), mL	5.4 (2.2–15.3)
Median onset time to first scan (IQR), hours	30.1 (12.8–66.6)

SD = standard deviation; IQR = interquartile range; NIHSS = National Institute for Health Stroke Scale.

freedom in FMRIB's Linear Image Registration Tool.[26] All the registration results were inspected by T.W.

Statistical Analysis

GROUP COMPARISON. The metabolite concentrations were calculated relative to the sum of contralateral NAA, creatine, and choline signals for each patient. The acute-to-subacute stage comparisons were performed among three time windows, that is, 0–24 hours (N = 32), 24 hours to 1 week (N = 47) and 1–2 weeks (N = 19).[3,27] Linear mixed effects modeling analysis was used for the comparison of lesional neurometabolites across the above three time windows to account for repeated measurements.[28] The comparisons were repeated by using longitudinal data only (the 25 patients data with repeated MRI scans only). Both linear mixed-effects modelling analysis incorporating all the data and paired t-tests across different time windows were performed. The hyperacute stage comparisons were performed between early and late hyperacute windows, that is, 0–6 hours (N = 11) and 6–24 hours (N = 21) post onset, using independent samples t-tests applied to only cross-sectional data (i.e. first scan data of the 32 patients within hyperacute window).

CORRELATION AND REGRESSION ANALYSIS. The relationship between neurometabolite concentrations and time after stroke onset or lesion volume in the hyperacute stage was examined with Pearson correlation analyses. In addition, Bayesian logistic ridge regression was performed to compare the capability of discriminating the onset windows— early hyperacute (<6 hours) vs late hyperacute (6–24 hours)—by using 1) NAA, 2) NAA, and Cho, 3) NAA, Cho, and Cr, 4) NAA, Cho, Cr, and Lac as inputs data, respectively. The widely applicable information criterion (WAIC) was used for model comparison gracefully weighting goodness-of-fit against model complexity.[29] Receiver operator characteristic (ROC) analysis was performed to compare the classification performance of the above four models. The area under the curve (AUC) was compared between four models using the combination of different biomarkers. The statistical analyses were performed using SPSS (version 27.0; IBM, Armonk, NY, USA). The Bayesian analysis was implemented with Bayesreg in MATLAB (version R2021b; MathWorks, Natick, MA, USA).[30] $P < 0.05$ was considered statistically significant.

Results

Demographic information of the 73 patients is listed in Table 1. The mean age was 65 ± 14 years. On admission prior to the MRI scans, the patients were assessed on the National Institutes of Health Stroke Scale (NIHSS), with a median score of 4 (IQR, 3–8). The median DWI- or FLAIR-based core lesion volume was 5.4 (IQR, 2.2–15.3) mL. Figure 1 shows a set of tri-planar NAA images and the
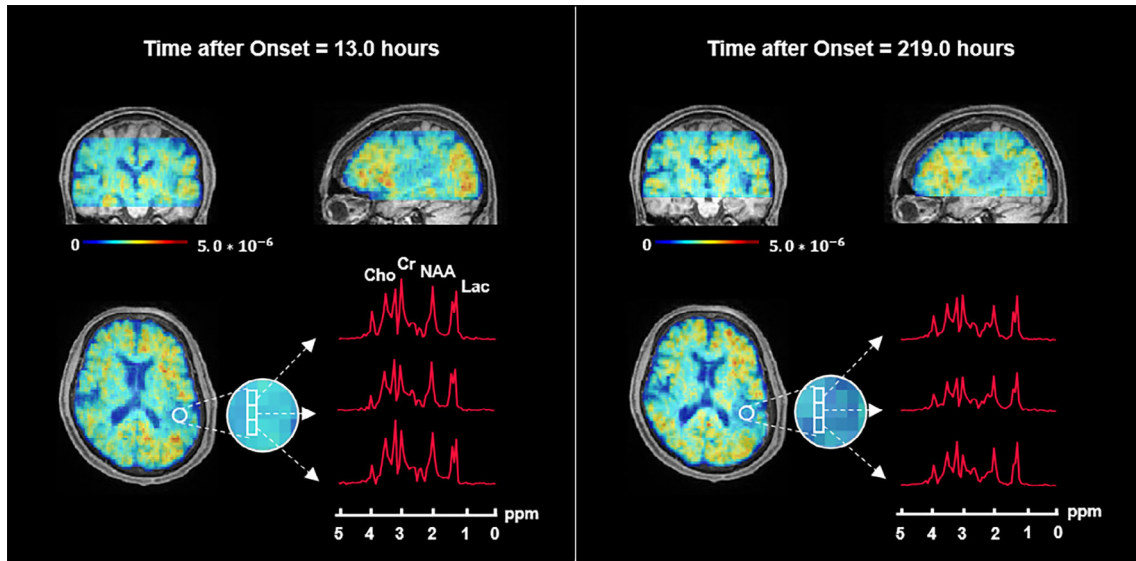
FIGURE 1: 3D N-acetylaspartate (NAA) maps and representative spectra from the ischemic lesion of a stroke patient scanned repeatedly at 13.0 hours and 219.0 hours after symptom onset, respectively. The NAA maps in triplanar views are registered to and overlaid on T1-weighted images.

FIGURE 2: Multimodal images from representative patients at 2.3–108.5 hours after ischemic stroke. The ischemic lesions were depicted in red on DWI images. All images (DWI, FLAIR, NAA, choline, creatine, and lactate) were registered to the structural T1-weighted images. The color bar for MR spectroscopic imaging (MRSI) shows neurometabolite level in institutional units, for which the MRSI metabolite measurements were normalized over the companion unsuppressed water signals.

4

representative MRSI spectra in the area of the lesion, which were acquired from the same patient scanned at 13.0 hours and 219.0 hours post stroke onset. The spectra acquired at the later time point showed noticeably reduced NAA peaks. Representative neurometabolite maps from
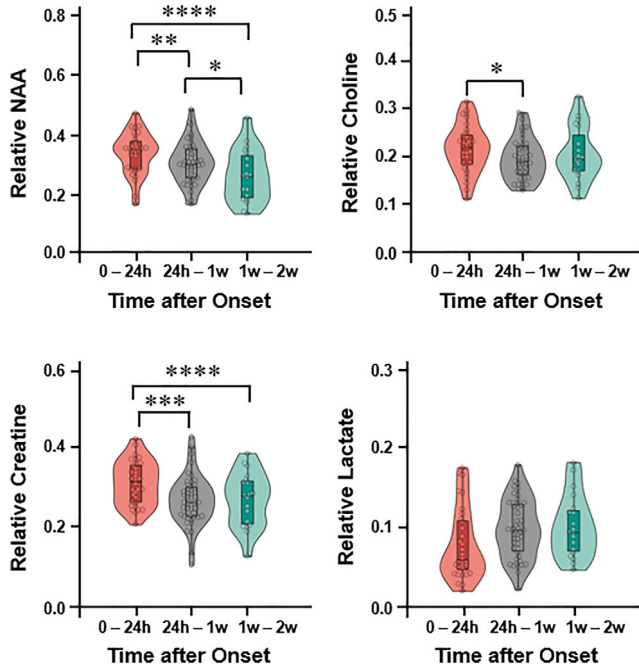
six different ischemic stroke patients with onset time from 2.3 to 108.5 hours are shown in Figure 2 in the order of increasing time after onset, along with the corresponding DWI and FLAIR images. Reduced NAA signal intensity and enhanced lactate signal intensity within the lesion compared to the contralateral side can be observed, as well as an inverse relationship between NAA signal and onset time.
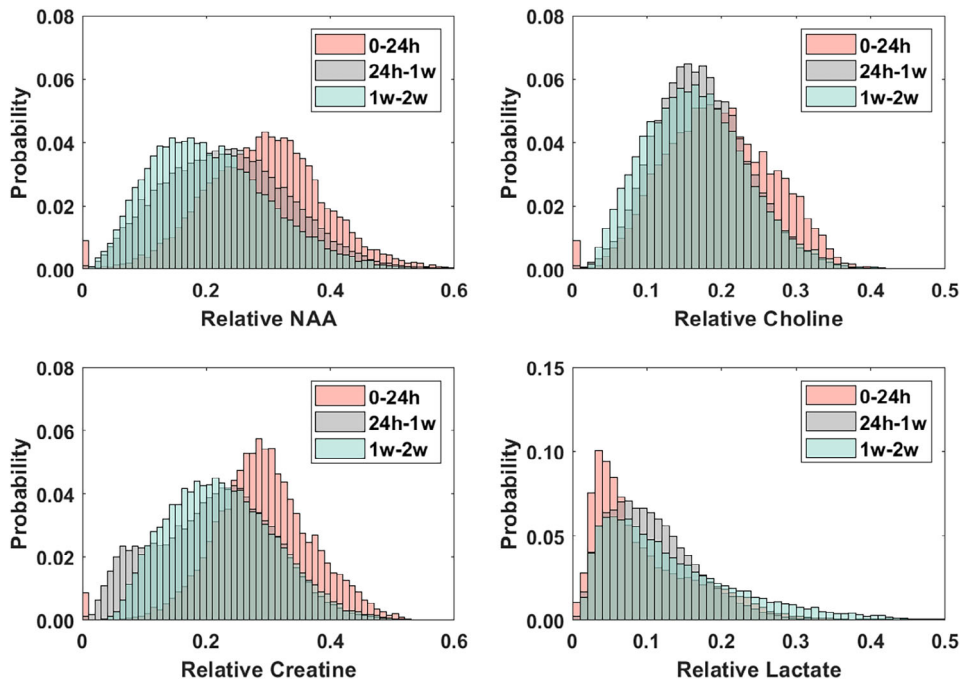
Figure 3 shows the acute-to-subacute group comparisons. The NAA concentration of the 0–24 hours group was significantly higher than that of the 24 hours to 1 week group, which in turn was significantly higher than that of the 1–2 weeks group. About 22% reduction in NAA was observed from 1 day to 2 weeks after stroke onset. The creatine concentration of the 0–24 hours group was significantly higher than that of the 24 hours to 1 week group and the 1–2 weeks group. The choline concentration of the 0–24 hours group was significantly higher than that of the 24 hours to 1 week group. The main effects of time were shown on NAA ($F = 14.321$) and creatine ($F = 12.261$). When including longitudinal data only, that is, the 25 patients data with follow-up scans, the main effects of time were similarly found on NAA ($F = 13.394$) and creatine ($F = 11.972$). For the patients from 0–24 hours to 24 hours to 1 week windows ($N = 7$), lesional NAA and creatine significantly decreased. For the patients from 0–24 hours to 1–2 weeks windows ($N = 9$), lesional NAA and creatine were also significantly decreased. Altogether, the NAA and creatine were consistently decreased from hyperacute to acute or subacute stages, which also showed main effects of time. Voxel-wise neurometabolic

FIGURE 3: Comparisons of the neurometabolite concentrations within ischemic lesion of acute and subacute ischemic stroke patients at 0–24 hours, 24 hours to 1 week, and 1–2 weeks after symptom onset. Error bars represent 95% confidence intervals. *$P < 0.05$; **$P < 0.01$; ***$P < 0.001$; ****$P < 0.0001$.

FIGURE 4: Histograms of voxel-wise neurometabolites concentrations in the ischemic lesion across all stroke patients at 0–24 hours, 24 hours to 1 week, and 1–2 weeks post-symptom onset, respectively.
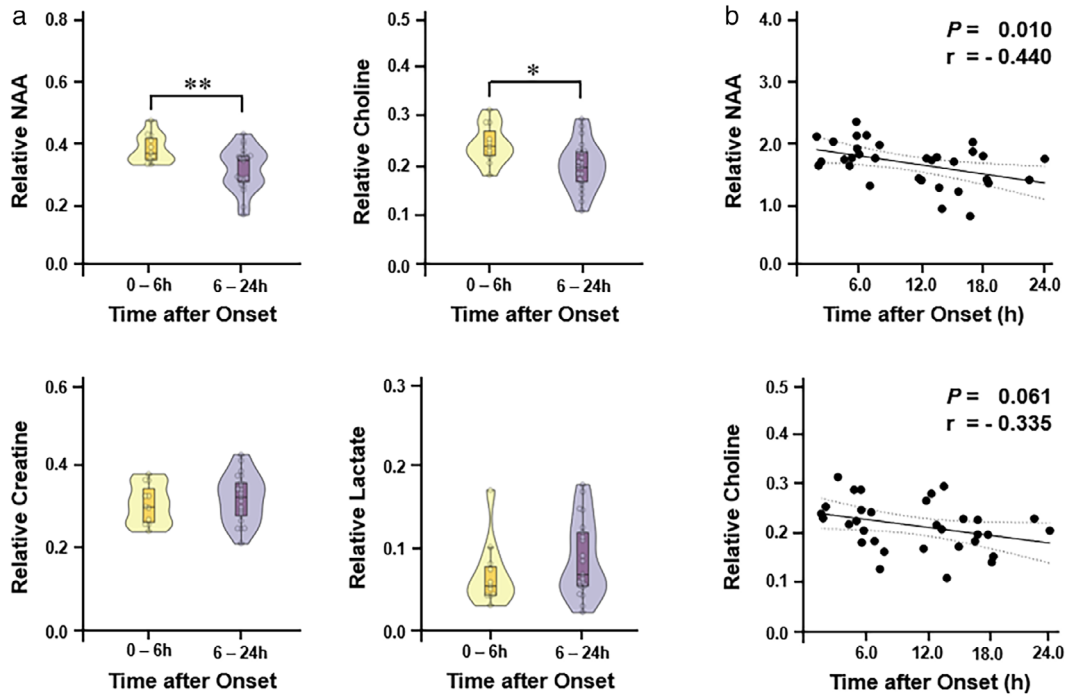
FIGURE 5: (a) Comparisons of neurometabolite concentrations within DWI lesion in hyperacute ischemic stroke patients at 0–6 hours and 6–24 hours after symptom onset. Error bars represent 95% confidence intervals. **$P < 0.01$; *$P < 0.05$. (b) NAA concentration decreased with time after onset within the first 24 hours post stroke. Dashed lines represent 95% confidence interval of fit.
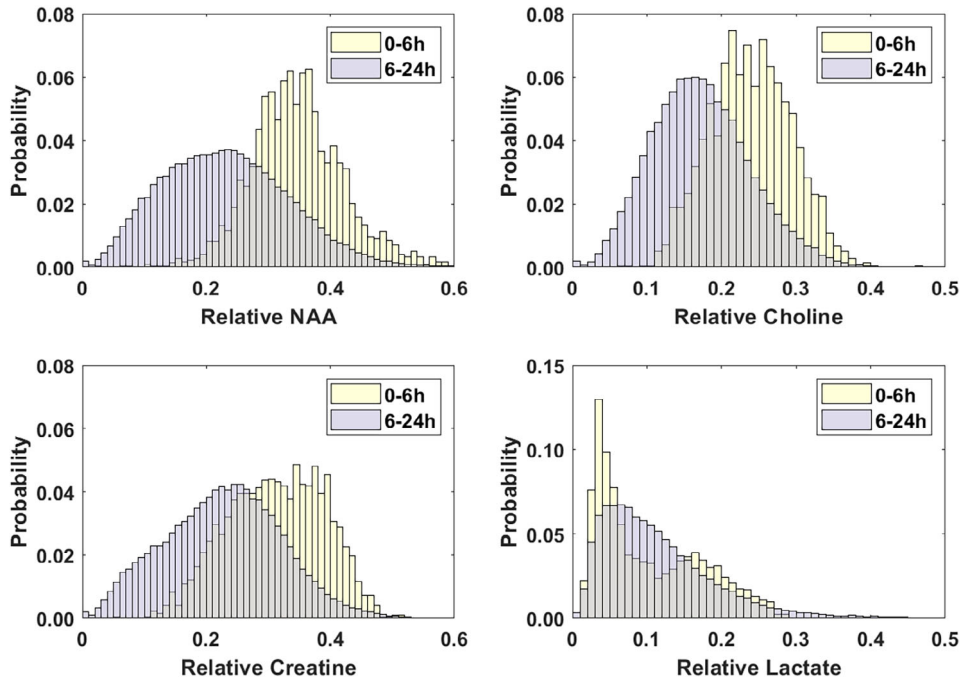
FIGURE 6: Histograms of voxel-wise neurometabolites concentrations within DWI lesion between early (0–6 hours) and late (6–24 hours) hyperacute stroke patients.

signal measurements across all patients are shown in Figure 4. These plots show not only the changes of mean lesional neurometabolites concentrations but also increase in the variation of the signals from hyperacute to acute and subacute groups.

All the hyperacute stage data (<24 hours, $N = 32$) were cross-sectional. Figure 5a shows the comparisons between the 0–6 hours (i.e. early hyperacute) and 6–24 hours (i.e. late hyperacute) groups. The NAA and choline concentrations of

the early hyperacute group were higher than that of the late hyperacute group. Within the first 24 hours, the NAA level decreased with increased time post onset in ischemic stroke patients ($r = -0.440$) but not for the other metabolites (choline: $r = -0.335$, $P = 0.061$; lactate: $r = 0.069$, $P = 0.709$; creatine: $r = -0.023$, $P = 0.900$), as shown in the scatter plots of Figure 5b. These results remained true even after controlling for age and lesion volume (NAA: $r = -0.437$; choline: $r = -0.325$, $P = 0.085$; lactate: $r = 0.044$, $P = 0.820$; creatine: $r = 0.025$, $P = 0.899$). No between-group differences were found in lactate and creatine concentrations (lactate: $P = 0.256$; creatine: $P = 0.550$). The decrease of NAA and increase of lactate concentration were correlated with lesion volume (NAA: $r = -0.472$; lactate: $r = 0.366$) but not for choline and creatine. Figure 6 showed the voxel-wise neurometabolites concentrations between early and late hyperacute patients. The NAA and lactate signals were more variable in the late hyperacute group compared to the early hyperacute group, indicating increased neurometabolic heterogeneity within the lesion. Taken together, we showed that the lesional NAA concentration served as the most sensitive biomarker of time post symptom onset in hyperacute stroke patients.

Figure 7 shows the ROC curves that evaluate the extent to which the neurometabolites measurements obtained by MRSI could discriminate between 0–6 hours and 6–24 hours groups in hyperacute stroke patients. Group separation using combined neurometabolites including NAA, creatine, and choline yielded an AUC of 0.90 (95% confidence interval [CI] = 79%–100%; WAIC: 16.51). This model also exhibited the lowest WAIC, indicating the best balance of flexibility and fit. It is noted that adding the
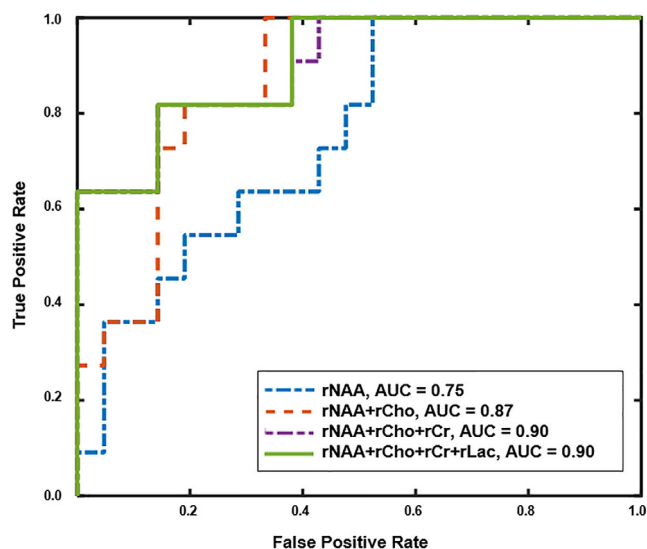
FIGURE 7: Receiver operating characteristic curves of Bayesian logistic ridge regression for separation between early (0–6 hours) and late hyperacute (6–24 hours) ischemic stroke patients.

lactate signal did not improve the separation performance, which yielded an AUC of 0.90 (95% CI = 80–100%; WAIC: 17.70).

Discussion

In this study, we applied fast high-resolution 3D MRSI to reveal temporal changes of neurometabolites in human ischemic stroke at multiple time scales. We found that the NAA and creatine concentrations in the ischemic lesion reduced from acute to subacute stroke patients. Our results revealed that the NAA concentration within the DWI lesion was correlated with post-onset time within the hyperacute stage (<24 hours) of ischemic stroke patients. We also showed that the discrimination capability between early hyperacute (<6 hours) from late hyperacute (6–24 hours) stage patients was improved when incorporating NAA, choline, and creatine. As a noninvasive neurometabolic imaging technique, the potential of MRSI has long been recognized for identifying salvageable ischemic tissue and revealing the metabolic changes during brain ischemia and ongoing tissue injury.[8–12,14,15,24,25,31–38]

The first serial MRS study in 1990 of ischemic stroke patients at 3 days to 10 weeks post onset[12] stimulated interest in assessing neurometabolic signal changes within the ischemic brain tissue during stroke progression. However, early MRSI techniques, such as single-voxel MRS or 2D MRSI, are limited by the low spatial resolution, long acquisition time, and partial coverage of the tissue. These limitations had impeded their clinical use for stroke imaging. Building on the previous work,[11] in this study, we leveraged high-resolution 3D MRSI imaging on a cohort of ischemic stroke patients across both acute and subacute stages. Spatial maps of multiple neurometabolites including NAA, lactate, choline, and creatine were acquired at $2.0 \times 3.0 \times 3.0$ mm^3 nominal resolution, allowing good delineation of their concentrations within the whole lesion area and minimizing the influence of the partial volume effects.

We revealed that NAA concentrations seem to be sensitive to the progression of ischemic damage in stroke. NAA, one of the most prominent signals in brain MRS data, is a marker of the functional integrity of neuronal mitochondrial metabolism[25]. In ischemic stroke, the reduction in NAA concentration within the lesion has been a consistent observation, indicating neuronal/axonal loss or mitochondrial dysfunction. Hours after stroke onset, rapid decreases in NAA within the infarct core have been detected in both human and animal studies,[14,24] generally attributed to neuronal damage. Our work showed a decline in NAA concentration (about 17.5%) from the early (<6 hours) to late hyperacute (6–24 hours) phases, close to the findings in previous study which observed about 24% decline in NAA from 0–6 hours to 6–24 hours[31]. More importantly, we reveal a linear correlation between

NAA concentration and onset time within the first 24 hours of a stroke.

Dani et al. have investigated neurometabolite concentrations in ischemic tissue within 24 hours of onset in ischemic stroke with single-slice multivoxel MRS,[14] reporting a 10.6% difference in NAA between the early and late hyperacute patients identically grouped as in our study. The discrepancy with our results might be related to the inclusion of merely hypo-perfused tissue arising from the limited spatial resolution (>10 mm). Such partial volume effects are substantially reduced by the high-resolution achieved with SPICE, improving the sensitivity for detecting subtle changes in neurometabolic signals of pathological brain tissues. We also observed a significant decrease in NAA from acute to subacute stages, consistent with the findings of a previous longitudinal study.[10] The further decline of NAA from acute to subacute stages has been attributed to accumulating neuronal damage, which continues up to 12 days postischemic stroke in humans.[10,34]

Creatine and phosphocreatine are markers of energy metabolism in neuronal and glial cells, constituting a cellular energy buffering and phosphate transport system.[6] In our current study, creatine did not show significant reduction from early to late hyperacute time windows but did show a sustained decrease from hyperacute to acute as well as subacute time windows. In line with this, other studies have consistently found a general decrease of creatine in the ischemic lesion from acute stage till up to 3 months after stroke.[10,15] The vulnerability to hypoxia is different for different cell types. In the rodent stroke model, delayed depletion of creatine was found following NAA depletion after permanent occlusion.[24] The greater and more rapid reduction in NAA level in infarction may indicate a higher susceptibility to ischemia for neurons. Creatine is present in both neurons and glial cells, and glial cells are known to be more resistant to ischemia.[39] This issue might explain the observation of delayed reduction in creatine concentrations within the infarction in our work and in previous studies.[33,34]

Choline is a marker of cellular membrane turnover, through its involvement in membrane synthesis and degradation.[38] Previous findings about the changes of choline concentrations in stroke range from no difference,[12] increased[35] or decreased[32] choline levels within stroke lesions. Discrepancies might be related to individual variability, various time windows post onset and small sample size. Our work found decreased lesional choline concentrations in hyperacute and acute stages but not in subacute stage of stroke patients. These findings are in line with previous longitudinal study that showed a reduced choline level within the lesion during the first 2 weeks but not over 3 months in stroke.[10] More interestingly, a decreased choline signal from early to late hyperacute stroke was observed, which might be due to the disrupted metabolic pathway for the membrane maintenance due to the energy breakdown post occlusion.

Dynamic lactate changes in ischemic stroke are variable in literature. A reduction of lactate in the DWI lesion from 1 to 5 days post symptom onset has been shown in a longitudinal study of ischemic stroke patients.[10] On the other hand, persistently elevated lactate signals within the infarction have been shown weeks or even months after stroke.[35,36] In this study, a large variability was found in lactate concentrations across different patients within different time windows post stroke onset, leading to nonsignificant group differences. The lactate production within hyperacute stage post stroke onset mainly reflects the anaerobic glycolysis in potentially viable neurons or glia cells.[34] In the later stage of stroke, elevated lactate signals have been attributed to infiltrating inflammatory cells such as macrophages, which begin to appear at 3 days post infarction and gradually disappear over months.[10,36] This might also explain the persistence of lactate signals into the chronic stage.[37] The time course of acidosis due to ischemia and its spontaneous clearance are critical to cell death.[35] Therefore, the lactate level within the acute DWI-defined lesion has provided prognostic information for both clinical outcome and final infarct size in stroke patients.[18,36] In our work, higher lactate concentrations were correlated with larger infarct volume in hyperacute stroke patients. The lactate signal might not provide a reliable biomarker for time post onset assessment because of its complicated pathological processes, which result in the continuous signal elevations across different stages of stroke.

Limitations

This study requires validation with a larger and more diverse samples covering a wider range of time points, especially in the critical early period. Longitudinal data were severely limited in the current study. The inclusion of patients with a relatively narrow range of presenting deficit (NIHSS ≤12) increase the chance of type I error and underestimate the effect of association between the imaging measures and onset time. Exploration of a wider range of deficits would be desirable, as far as local imaging procedures enable MR imaging to be delivered safely within the clinical stream. Further work is required to contextualize the metabolic maps by perfusion imaging, which would reveal inter-individual differences in the degree of ischemia that are bound to interact with the extent of metabolic distress. Finally, given the considerable heterogeneity of ischemic stroke patients, variation with factors such as lesion anatomy and degree of perfusion deficit or reperfusion should be surveyed across their full range.[40]

Conclusion

This study shows that the neurometabolite concentrations within the ischemic lesion might be time-dependent in stroke

patients. The changes of neurometabolites seem to provide good discrimination between ischemic stroke patients for early and late hyperacute (i.e., before and after 6 hours) time windows. Fast 3D MRSI provides a clinically feasible tool for the assessment of neuronal and glia cell loss postischemic stroke.

Conflict of Interest

None of the authors declare any conflict of interest pertinent to the present work.

REFERENCES

1. Powers WJ, Rabinstein AA, Ackerson T, et al. 2019 update to the 2018 guidelines for the early management of acute ischemic stroke: A guideline for healthcare professionals from the American Heart Association/American Stroke. Stroke 2019;50:344-418.

2. Berner LP, Cho TH, Haesebaert J, et al. MRI assessment of ischemic lesion evolution within white and gray matter. Cerebrovasc Dis 2016; 41:291-297.

3. Allen LM, Hasso AN, Handwerker J, Farid H. Sequence-specific MR imaging findings that are useful in dating ischemic stroke. Radiographics 2012;32:1285-1297.

4. Albers GW, Marks MP, Kemp S, et al. Thrombectomy for stroke at 6 to 16 hours with selection by perfusion imaging. N Engl J Med 2018;378: 708-718.

5. Nogueira RG, Jadhav AP, Haussen DC, et al. Thrombectomy 6 to 24 hours after stroke with a mismatch between deficit and infarct. N Engl J Med 2018;378:11-21.

6. Prass K, Royl G, Lindauer U, et al. Improved reperfusion and neuroprotection by creatine in a mouse model of stroke. J Cereb Blood Flow Metab 2007;27:452-459.

7. Brouns R, Deyn D. The complexity of neurobiological processes in acute ischemic stroke. Clin Neurol Neurosurg 2009;111:483-495.

8. Gillard JH, Barker PB, Zijl PC, Bryan RN, Oppenheimer SM. Proton MR spectroscopy in acute middle cerebral artery stroke. Am J Neuroradiol 1996;17:873-886.

9. Barker PB, Gillard JH, Zijl PC, et al. Acute stroke: Evaluation with serial proton MR spectroscopic imaging. Radiology 1994;192:723-732.

10. Muñoz MS, Cvoro V, Chappell FM, et al. Changes in NAA and lactate following ischemic stroke: A serial MR spectroscopic imaging study. Neurology 2008;71:1993-1999.

11. Li Y, Wang T, Zhang T, et al. Fast high-resolution metabolic imaging of acute stroke with 3D magnetic resonance spectroscopy. Brain 2020; 143:3225-3233.

12. Fenstermacher MJ, Narayana PA. Serial proton magnetic resonance spectroscopy of ischemic brain injury in humans. Invest Radiol 1990;25: 1034-1039.

13. Muñoz MS, Cvoro V, Armitage PA, Marshall I, Bastin ME, Wardlaw JM. Choline and creatine are not reliable denominators for calculating metabolite ratios in acute ischemic stroke. Stroke 2008;39:2467-2469.

14. Dani KA, An L, Henning EC, Shen J, Warach S. Multivoxel MR spectroscopy in acute ischemic stroke: Comparison to the stroke protocol MRI. Stroke 2012;43:2962-2967.

15. Lanfermann H, Kugel H, Heindel W, Herholz K, Heiss WD, Lackner K. Metabolic changes in acute and subacute cerebral infarctions: Findings at proton MR spectroscopic imaging. Radiology 1995;196:203-210.

16. Wild JM, Wardlaw JM, Marshall I, Warlow CP. N-acetylaspartate distribution in proton spectroscopic images of ischemic stroke: Relationship to infarct appearance on T2-weighted magnetic resonance imaging. Stroke 2000;31:3008-3014.

17. Nicoli F, Lefur Y, Denis B, Ranjeva JP, Confort GS, Cozzone PJ. Metabolic counterpart of decreased apparent diffusion coefficient during hyperacute ischemic stroke: A brain proton magnetic resonance spectroscopic imaging study. Stroke 2003;34:e82-e87.

18. Cvoro V, Wardlaw JM, Marshall I, et al. Associations between diffusion and perfusion parameters, n-acetyl aspartate, and lactate in acute ischemic stroke. Stroke 2009;40:767-772.

19. Liang Z-P. Spatiotemporal imaging with partially separable functions. *2007 Joint Meeting of the 6th International Symposium on Noninvasive Functional Source Imaging of the Brain and Heart and the International Conference on Functional Biomedical Imaging.* Hangzhou, China: IEEE; 2007. p 181-182.

20. Lam F, Liang Z-P. A subspace approach to high-resolution spectroscopic imaging. Magn Reson Med 2014;71:1349-1357.

21. Lam F, Ma C, Clifford B, Johnson CL, Liang Z-P. High-resolution ^{1}H-MRSI of the brain using SPICE: Data acquisition and image reconstruction. Magn Reson Med 2016;76:1059-1070.

22. Ma C, Lam F, Johnson CL, Liang Z-P. Removal of nuisance signals from limited and sparse ^{1}H MRSI data using a union-of-subspaces model. Magn Reson Med 2016;75:488-497.

23. Li Y, Lam F, Clifford B, Liang Z-P. A subspace approach to spectral quantification for MR spectroscopic imaging. IEEE Trans Biomed Eng 2017;64:2486-2489.

24. Higuchi T, Fernandez EJ, Maudsley AA, Shimizu H, Weiner MW, Weinstein PR. Mapping of lactate and n-acetyl-l-aspartate predicts infarction during acute focal ischemia: In vivo ^{1}H magnetic resonance spectroscopy in rats. Neurosurgery 1996;38:121-129. discussion 129–130.

25. Moffett J, Ross B, Arun P, Madhavarao C, Namboodiri A. N-acetylaspartate in the CNS: From neurodiagnostics to neurobiology. Prog Neurobiol 2007;81:89-131.

26. Jenkinson M, Beckmann C, Behrens TEJ, Woolrich M, Smith S. FSL. NeuroImage 2012;62:782-790.

27. Bernhardt J, Hayward KS, Kwakkel G, et al. Agreed definitions and a shared vision for new standards in stroke recovery research: The stroke recovery and rehabilitation roundtable taskforce. Int J Stroke 2017;12: 444-450.

28. Chen G, Saad ZS, Britton JC, Pine DS, Cox RW. Linear mixed-effects modeling approach to fMRI group analysis. Neuroimage 2013;73: 176-190.

29. Watanabe S. A widely applicable Bayesian information criterion. J Mach Learn Res 2013;14:867-897.

30. Makalic E, Schmidt DF. High-dimensional Bayesian regularised regression with the Bayesreg package. arXiv 2016;arXiv:1611.06649.

31. Sager TN, Hansen AJ, Laursen H. Correlation between n-acetylaspartate levels and histopathologic changes in cortical infarcts of mice after middle cerebral artery occlusion. J Cereb Blood Flow Metab 2000;20:780-788.

32. Duijn JH, Matson GB, Maudsley AA, Hugg JW, Weiner MW. Human brain infarction: Proton MR spectroscopy. Radiology 1992;183: 711-718.

33. Zöllner JP, Hattingen E, Singer Oliver C, Pilatus U. Changes of pH and energy state in subacute human ischemia assessed by multinuclear magnetic resonance spectroscopy. Stroke 2015;46:441-446.

34. Saunders DE, Howe FA, Boogaart A, McLean MA, Griffiths JR, Brown MM. Continuing ischemic damage after acute middle cerebral artery infarction in humans demonstrated by short-echo proton spectroscopy. Stroke 1995;26:1007-1013.

35. Graham GD, Blamire AM, Howseman AM, et al. Proton magnetic resonance spectroscopy of cerebral lactate and other metabolites in stroke patients. Stroke 1992;23:333-340.

36. Parsons MW, Li T, Barber PA, et al. Combined ^{1}H MR spectroscopy and diffusion-weighted MRI improves the prediction of stroke outcome. Neurology 2000;55:498-506.

37. Petroff OA, Graham GD, Blamire AM, et al. Spectroscopic imaging of stroke in humans: Histopathology correlates of spectral changes. Neurology 1992;42:1349-1354.

38. Miller BL. A review of chemical issues in ^{1}H NMR spectroscopy: N-acetyl-l-aspartate, creatine and choline. NMR Biomed 1991;4:47-52.

39. Kolpakova ME, Veselkina OS, Vlasov TD. Creatine in cell metabolism and its protective action in cerebral ischemia. Neurosci Behav Physiol 2015;45:476-482.

40. Bonkhoff AK, Xu T, Nelson A, et al. Reclassifying stroke lesion anatomy. Cortex 2021;145:1-12.